ISSN: 2277-3754
ISO 9001:2008 Certified
International Journal of Engineering and Innovative Technology (IJEIT)
Volume 4, Issue 9, March 2015

White Light Generation by Electroluminescence for ZnO Nanoparticle –Organic Hybrid Junction Device

Abdulla M.Suhail*, Wasan R. Saleh*, Omar A. Ibrahim*, Rawa K. Ibrahim**
*Physics Department, College of Science, University of Baghdad, Iraq
** Ministry of Science and Technology, Advanced Material Research department, Iraq

Abstract-The ZnO organic hybrid junction (electroluminescence EL device) was fabricated using phase segregation method. ZnO-nanoparticle (NPs) was prepared as a colloidal by self–assembly method of Zinc acetate solution with KOH solution. Nanoparticle is employed to form organic-inorganic hybrid film and generate white light emission, while N,N'–diphenyl-N,N' –bis(3-methylphenyl)-1,1'-biphenyl 4,4'-diamine (TPD) and polymethyl methacrylate (PMMA) are adopted as the organic matrices. ZnO NPs was used to fabricate TPD: PMMA: ZnO NPs hybrid junction device. The photoluminescence (PL) and electroluminescence (EL) spectra of the TPD: PMMA: ZnO NPs hybrid device provided a broad emission band covering entirely the visible spectrum (~350-~700nm). The hybrid device gives a white emission attributed to the ZnO NPs intrinsic defects. Hence, white light emission can be achieved in a ZnO-organic hybrid device using low cost and low temperature growth techniques for both organic and inorganic materials.

Keywords: **electroluminescence, white light, ZnO, Nanoparticles.**

I. INTRODUCTION

Zinc Oxide (ZnO) has substantive advantages including the quests for LEDs [1], because of it wide band gap (3.37 eV) and large exciton binding energy (60 mV). Deep levels defects in ZnO can lead to an emission band different colors covering the whole visible spectrum. Such property makes ZnO, based white light emitting diodes [2]. The applications of ZnO to homojunction diodes has been limited due to the difficulties of high quality ZnO fabrication and p-doping on ZnO [3]. The difficulty of p-ZnO fabrication comes from ZnO has a very high ionization potential (~8eV) and electron affinity (~4.7eV) [4]. As an interesting alternate, the deposition of n-ZnO nanoparticle on different p-type semiconductors is quite frequent to utilize the electronic and optical advantages offered by heterostructure device [1]. Embedding semiconductor (dielectric) nanocrystals in organic matrices has created hybrid junction (EL device). The embedding dielectric nanoparticles in organic light emitting hybrid junction influences the luminescence spectra, because the energy of the lowest unoccupied molecular orbital (LUMO) and the highest occupied molecular orbital (HOMO) of the TPD polymer is nearest to the energy level of the embedded semiconductor, so an energy transfer will happen and also the electronic polarization of its environment. If the dielectric inclusions have stronger polarization than the polymer matrix, the EL spectrum of the dielectric/polymer hybrid film will has red-shifts compare with PL to the same dielectric material [5]. In this work, ZnO NPs was used to fabricate TPD: PMMA: ZnO NPs hybrid junction device by a spin coating method and study their EL and PL properties. A light emitting layers of ZnO NPs is obtained using a phase-segregation technique. The method followed in this work represents low cost and simple solution process without the need for sophisticated vacuum equipment to fabricate ZnO-based device [6].

II. EXPERIMENTAL WORK

All materials used to synthesis were supplied from Fluka Company, only the N, N'-diphenyl-N,N'-bis(3-methylphenyl)-1,1'-biphenyl-4,4'-diamine (TPD) was supplied by American Dye Source (Canada).

A. Synthesis of ZnO Nanoparticles

The NPs of ZnO were prepared as a colloidal by self–assembly method. For the synthesis of the ZnO NPs, 0.01M of Zinc acetate dehydrate (Zn $(CH_3COO)_2 .2H_2O$) solution was prepared by dissolved 1.25mmol of zinc acetate in 125ml of methanol under vigorous stirring at about 60^0C. Subsequently, a 0.03M of potassium hydroxide (KOH) solution was prepared by dissolved 2mmol of KOH in 65ml of methanol. KOH solution was added drop wise to zinc acetate solution and the reaction mixture was stirred for 2h at 60^0C [7]. In order to synthesis quantum dots more regular, the pH of mixture was (8.5). The transparency color of zinc acetate solution will start to change to the white after added the KOH solution. After 1h, the color will change to transparent white which indicate the starting of synthesis ZnO. After 2h the color will be opaque white which means that the amounts of formed ZnO NPs start increasing. The formed ZnO NPs can be separated by using the centrifugation and stored in ethanol. After that the sample was annealed at 300^0C. The fact that upon proper post-growth annealing, the hydroxyl group (OH) can desorbs and hence modify the emission from that of the as-grown ZnO nanostructure and lessening the lattice strain [8].

ISSN: 2277-3754
ISO 9001:2008 Certified
International Journal of Engineering and Innovative Technology (IJEIT)
Volume 4, Issue 9, March 2015

B. Preparation of PTD:PMMA:ZnO NPs hybrid junction device

Polymethyl methacrylate (PMMA) polymer was adopted a host matrix in the TPD: ZnO NPs mixture to provides a transparent host matrix for our organic-inorganic hybrid film. PMMA was used due to the good conductivity of TPD [5].

Addition of TPD to the ZnO NPs to achieve phase – segregated. As well as TPD serves as the hole transporting material in this inorganic-organic system, lead to increase the ZnO emission. This possibility suggests the combination of ZnO NPs and organic polymer electrode to form a hybrid lighting technology that avoids the problems associated with p-type ZnO. The TPD enhance electrons and holes to recombine in the ZnO NPs [9].

Finally adopt ZnO NPs, because it contains most of native defects introduce deep levels emission (DLE) at different positions in the band gap, and hence a rather large number of luminescence lines with different energies can be observed. This explains why all of the visible colors have been experimentally observed in different ZnO NPs samples. The common bands observed in ZnO are blue, green, and red luminescence DLE bands. Therefore ZnO nanostructure can be used in the white light generation [10].

The film fabrication started by cleaning the Indium Tin Oxide (ITO) glass substrate with acetone and iso-propanol under sonication for 5min. The ZnO NPs, TPD, and PMMA are dissolved in either chloroform separately. The TPD and PMMA solutions were prepared by dissolving 70mg/ml for each one separately in chloroform. Two ratios of (TPD:PMMA:ZnO NPs) were taken (1ml:1ml:0.5wt%) and (1ml:1ml:0.5wt%). The hybrid film was prepared by deposited the solution on the ITO coated glass substrate by spin-coating at 2500rpm for 20 s and annealed below 60^{o}C for 2 hours to remove the solvent.

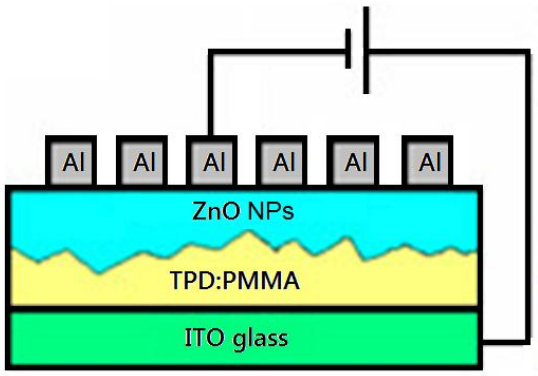

Fig (1): Structure of ZnO hybrid EL device

The hybrid film thickness was 1.2 µm. Afterwards, aluminum cathode is deposited on the hybrid film by evaporation process. The hybrid junction device is thus sandwiched between the ITO and the aluminum electrodes to fabricate EL device. Figure (1) shows the structure of the fabricated ZnO EL device. As a result of phase segregation, the ZnO NPs distribute in a layer above the TPD: PMMA film. The phase segregation occurs because the solubility of ZnO nanoparticles in chloroform is different from that of TPD: PMMA, which can then segregate from them during spin coating.

III. RESULTS AND DISCUSSION

The crystal graphic orientation of the ZnO NPs was analyzed by using a Shimadzu 6000 X-ray diffractometer using Cu kα radiation of wavelength 1.5406 A^{o}. XRD pattern was recorded at a scanning rate of 0.08333^{o} s^{-1} in the 2θ range from 30^{o} – 70^{o} as given in figures (2).

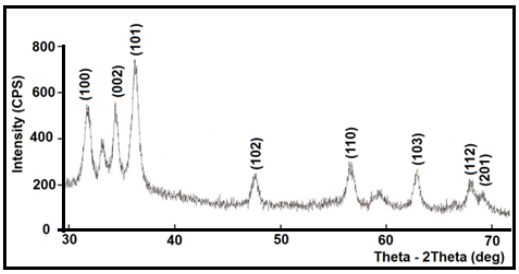

Fig (2): X-ray diffraction of ZnO NPs

The figure shows that the prepared ZnO NPs have polycrystalline structure. It is clear that the formed nanoparticle have wurtzite structure. It is obvious that the XRD pattern appears many diffraction peaks and strong orientation peak at 2θ = 36.28^{o} which is belong to (101) diffraction line.

The structure morphology for the samples was analyzed by using VEGA3 TESCAN, high vacuum mode SE from TESCAN ORSAY HOLDING, while the morphology surface analysis was carried out by employing CSPM AA3000 PFM supplied by Angstrom Company. Figure (3) show images of SEM at magnification of 50 Kx for the prepared ZnO NPs. The image reveals that the shape of formed nanoparticle is approximately spherical, while the inset image shows aggregation of nanoparticle in the range of 200 nm.

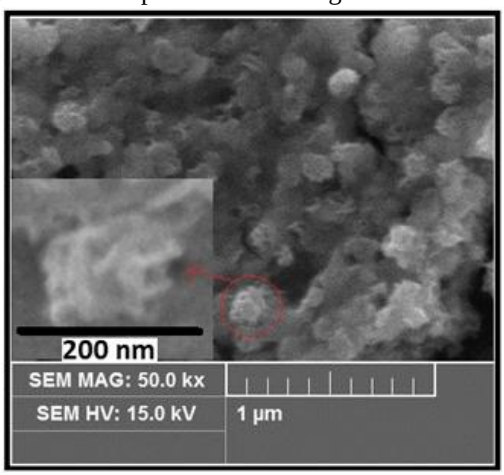

Fig (3): SEM images of ZnO nanoparticles; the inset image shows the aggregation of ZnO NPs.

ISSN: 2277-3754
ISO 9001:2008 Certified
International Journal of Engineering and Innovative Technology (IJEIT)
Volume 4, Issue 9, March 2015

To remove the aggregation, dissolved the ZnO NPs in chloroform solution and deposited on the glass slides. Figure (4) shows the ZnO NPs after remove the aggregation.

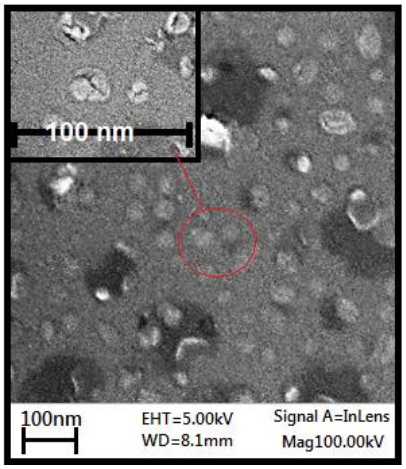

Fig (4): SEM images of ZnO NPs after removed the aggregation after removed the aggregation.

Figure (4) reveals that, after removed the aggregation, the shape of formed nanoparticle is approximately spherical in the range of 20 nm (this value is grain size), while the inset image shows the grain size contains many crystal in the range 10nm. This is the variance between the grain size and crystal size. The size calculated from X-ray diffraction pattern and Scherrer's relation is represents the crystal size which was equal to 9nm.

The absorbance of the samples was measured by LABOMED.INC spectra UV/Vis double beam scanning, covering range from (190 – 1100) nm.

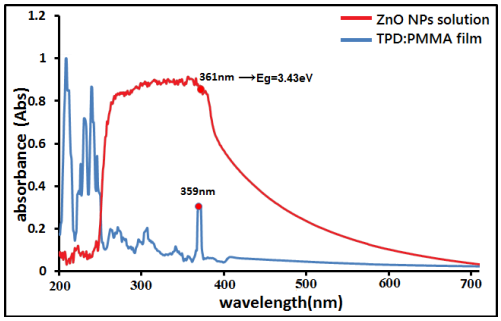

Fig (5): The absorbance spectrum PTD: PMMA hybrid film and ZnO NPs

The absorbance spectrum as a function of the wavelength in the range (190 – 700) nm for ZnO nanoparticles and TPD: PMMA are shown in figure (5). It is clear that the TPD: PMMA film has absorbance in the UV region. Where the peak 359nm related to TPD, which indicate that, the TPD: PMMA film was transparent in the visible region. Spectrum of ZnO NPs revealed that ZnO NPs have high response in the UV region and decreases exponentially with the increasing of wavelength in the visible region while ITO: glass spectrum is transparent at visible region.

This is mean that the emitted photons from ZnO will not suffer from any absorption during passing through the TPD: PMMA: ITO in the EL range 370-700 nm. This is except in the wavelength of 359nm were there is a peak of small absorption.

Figure (5) shows a prominent exciton band at 361nm corresponds to the ZnO NPs. This absorption peak is blue shifted as compared to the bulk exciton absorption of ZnO (373 nm), which is due to the size effect of the nanostructures. The high absorption band in the visible range of wavelength implies that exist more defect energy levels (trap stats or surface stats) in the synthesized ZnO NPs that are due to the specific experimental synthesis conditions according to [7].

The Photoluminescence spectrum was measured using VARIAN fluorescence spectrophotometer, supplied by Eclipse Company with the spectrum range from (190-1100) nm at room temperature. The photoluminescence spectrum of ZnO NPs excited by 300nm wavelength is shown in figure (6).

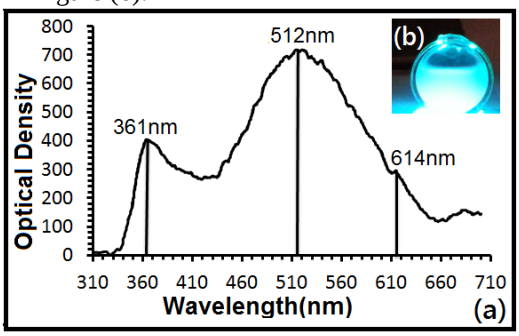

Fig (6): (a) PL spectrum of ZnO NPs and (b) the a photograph of ZnO NPs illuminate solution by UVGaN-LED.

Photoluminescence studies provide information of different energy deep states available between valance bands and conduction bands responsible for the irradiative recombination. These states are called trap states, which is caused the emission peaks. The origin trap states are came from intrinsic deep levels, this means native deep levels. The inset image shows the photograph of cyan light generation from illuminated ZnO NPs solution by UV GaN-LED. The energy band gap (Eg) and crystal size for ZnO NPs from PL spectrum calculated by using equations (1 and 2) and is found to be equal to 3.43 eV and 7.3 nm respectively.

$$E_g\,(eV) = \frac{1240}{\lambda(nm)} \qquad (1)$$

Crystal size (diameter=2r) was then calculated from energy gap using equation (2).

$$E_{NP} = Eg_{bulk} + \frac{\hbar^2\pi^2}{2er^2m_o}\left(\frac{1}{m_e} + \frac{1}{m_h}\right) - \frac{1.8e}{4\pi\varepsilon\varepsilon_o r} \qquad (2)$$

where: Eg_{NPs} is NPs band gap, Eg_{bulk} is the bulk band gap, m_e is the electron effective mass (=0.26 for ZnO), m_h is the hole effective mass (=0.59 for ZnO), e is the

ISSN: 2277-3754
ISO 9001:2008 Certified
International Journal of Engineering and Innovative Technology (IJEIT)
Volume 4, Issue 9, March 2015

electron charge, r is the radius of quantum dot, m_0 is the free electron mass, ε_0 is the permittivity of free space and ε is the relative permittivity.

The ZnO NPs film was electrically characterized using Hall Effect measurements. The film of 550nm thickness shows semiconductor of n-type behavior, which means that the charge carries are electrons.

A. Electrical properties of PTD:PMMA:ZnO NPs hybrid junction device

The electrical behavior of the hybrid junction device obtained using the TPD:PMMA:ZnO NPs. Figure (7) shows the I-V characteristics of the hybrid EL device. The figure reveals the rectification behavior with a turn-on voltage at bias voltage lower than 8 V. Light emission was detected at current levels of about 0.01-0.2 mA.

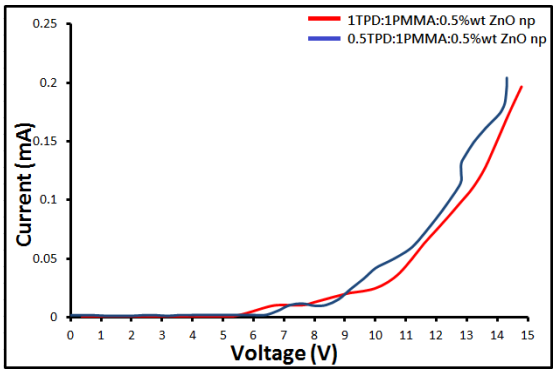

Fig (7): I-V characteristics of the hybrid EL device

The resulting I-V characteristics of ZnO: TPD: PMMA hybrid junction device analyzed using standard thermionic emission theory. According to this theory, the current in such device could be expressed as [11]:

$$I = I_s\left[exp\left(\frac{q(V - IR_s)}{nKT}\right) - 1\right] \qquad (3)$$

where Is is the saturation current, Rs is the series resistance, k is the Boltzmann constant, T is the absolute temperature, q is the elementary electric charge, V is the applied voltage, and n is the ideality factor.

Below the turn-on voltage, Rs decreases with increasing the forward bias, and then it maintains a constant value above the turn-on voltage .Under the forward bias the conduction band barrier will be decreased and will enhance the electron flow from the n-ZnO NPs to the p-TPD and holes from the p-TPD to the n-ZnO NPs. The successive recombination would give rise to the forward bias current flow. This means that the diode resistance would firstly decrease upon the increase of the forward bias voltage (i.e., the lowering of the barrier). As the forward bias is large enough, the barrier is negligible; the diode resistance (Rs) becomes constant [10]. No rise in the forward current under low bias could be explained that good contact between the Al electrode and ZnO NPs.

Two mechanisms influence the junction behavior, firstly ; the transport mechanism is no longer dominated by the thermionic emission that occur in higher value of the ideality factor, Second; mechanism it was occur non ideal behavior is often attributed to defect states in the band gap of the semiconductor providing other current transport mechanisms such as structural defects, surface contamination, barrier tunneling, or generation recombination in the space charge region and to variations in the interface composition.

To understand which mechanisms influence the junction behavior, the I-V characteristics of the device are drawn in figure (8) in a log-log scale for the ratio 1TPD:1PMMA:0.5%wt, because this ratio gave white light generation.

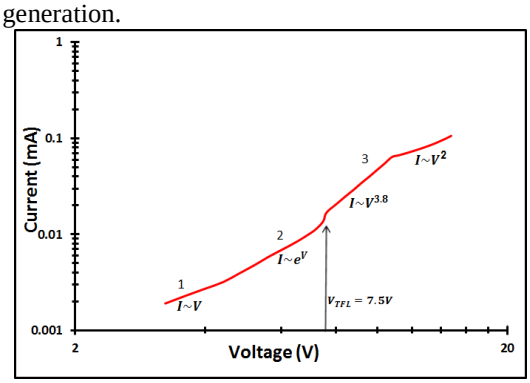

Fig (8): Log-log plot of the I-V characteristics of the 1TPD:1PMMA:0.5%wt ZnO NPs hybrid junction device

The log-log plot of the I-V data at RT is shown in figure (8) and it illustrates that the current transport mechanism is exhibited in three different regions. The current in region 1 follows a linear dependence, that is, I~V. This is an indication that the current transport is dominated by tunneling at low voltages. The boundary for this region was determined to be below 4.5V. In region 2 (4.5-7.5 V) the current increases exponentially as I~ exp (cV). The ideality factor (19) is determined in this region and the dominating transport mechanism is recombination tunneling. Finally above 8 V (region 3) the current follows a power law ($I \sim V^{3.8}$), indicating a space-charge-limited current (SCLC) transport mechanism. Space-charge-limited current and at least one of the other regions ($I \sim V^2$) observed in the present study have been reported in different n-ZnO /p- Si heterojunction and in Schottky contact to ZnO rods, this result and explanation was identical with P. Klassen [10].

According to the previous results, the EL spectra was studied in the forward biased voltage of 8 and 12V, because these voltages located at regions 2 and 3 respectively.

A. Electroluminescence properties of PTD:PMMA:ZnO NPs hybrid junction device

The EL measurements under forward bias voltages of 8 and 12V of the 1TPD:1PMMA:0.5%wtZnONPs and 0.5TPD:1PMMA:0.5%wtZnONPs hybrid junction

ISSN: 2277-3754
ISO 9001:2008 Certified
International Journal of Engineering and Innovative Technology (IJEIT)
Volume 4, Issue 9, March 2015

devices were carried out using a photomultiplier detector at room temperature. Figure (9) shows the corresponding EL spectrum for 1TPD:1PMMA:0.5%wt ZnO NPs samlpe under forwared bias voltage (8,12)V.

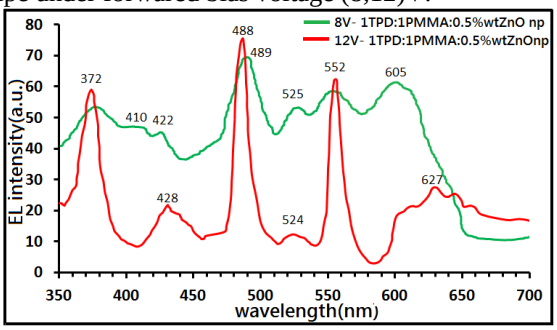

Fig (9): EL spectrum under forward bias voltage of 8 and 12V of the 1TPD:1PMMA:0.5%wt ZnO NPs

Studied the emission spectrum of figure (9) by CIE 1931 chromaticity diagram, indicate that the white light generated at forward bias voltage of 12V. Therefore another ratio was taken with the same voltage.

It is clear from the figure that the peak at 410nm was appeared of bias voltage 8V, but when increased to 12V, this peak disappeared. This is may be attributed to increasing of the diffusion current which reduces the production of excitons between C.B and HOMO level, where the holes speedily moving towards C.B of ZnO NPs

The EL spectrum of the 1TPD:1PMMA:0.5%wtZnO NPs and 0.5TPD:1PMMA:0.5%wtZnO NPs hybrid device under forward bias voltage 12V can see in figure (10).

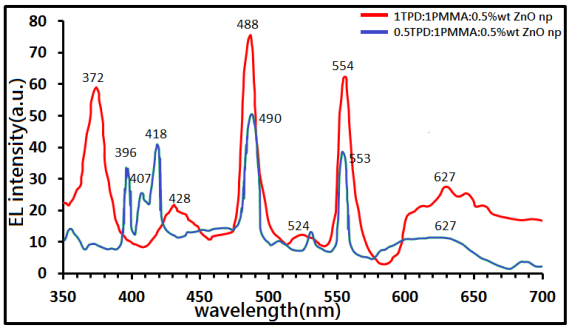

Fig (10): EL spectrum of the 1TPD:1PMMA:0.5%wtZnO NPs and 0.5TPD:1PMMA:0.5%wtZnO NPs hybrid device under forward biased voltage 12V.

The mechanism transport of carrier in our hybrid junction device is that, the TPD serves as the hole transporting material. Holes are injected from the ITO anode into the HOMO of the TPD matrix and transported to the valance band (V.B) or to the acceptor levels (V_{Zn} ,V_O, O_i, O_{Zn} and V_OZn_i) of the ZnO NPs. Meanwhile, electrons are injected from the Al cathode into the conduction band (C.B) or to the (Zn_i) of the ZnO NPs as shown in figure (11). Thus, holes and electrons from the excitons in the ZnO NPs and recombine radiatively these are called band-to-band recombination, and the holes and electrons recombination through defects to emission light in different wavelengths, this recombination through defects names the Shockley-Read-Hall (SRH) [12,13].

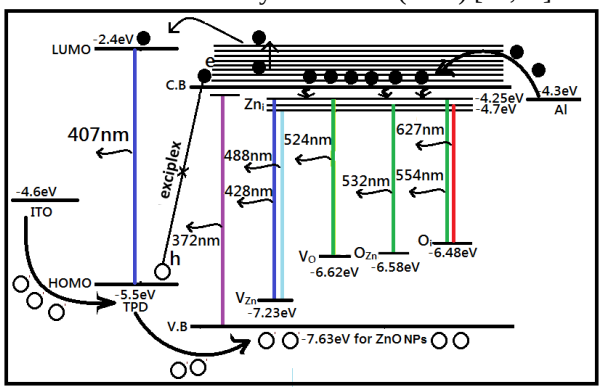

Fig (11): Energy bands diagram of TPD:PMMA:ZnO NPs hybrid device

The violet emission at 372nm is due to the band to band transition. The blue emission 428nm and cyan emission 488nm are corresponds to Zn_i to V_{Zn} transitions or Zn_i to acceptor level came from surface state in nanostructure effect. Green band centered at 2.36 eV (524nm) and attributed it to the oxygen vacancy (V_O), and green emission at 2.33 eV (532nm) has been attributed to the oxygen anti-site (O_{Zn}) while 2.24eV (554nm) green emission has been attributed to the oxygen anti-site (O_i). There is still controversy in the literature about the origin of the luminescence centers observed in ZnO materials [12,14]. The red emission at 2eV (627nm) is related to oxygen anti-site (Oi). All these transition are appear in figure (11).

In addition, new broad red-shifted components are found in the EL spectrum in figures (9) and (10) comparative with PL spectrum in figure (6). This may be attributed to the interaction between the TPD and ZnO nanocrystals. During spin-coating, the nanoparticles are embedded in the TPD film. Since the dielectric constant of the NPs is higher than that of the polymer, the dipoles in the inclusions are stronger than the surrounding polymer. The polarization of the inclusion is parallel to the dipole moment of the TPD molecules. The polarization energy of the TPD around the ZnO NPs hence diminishes. And since the LUMO-HOMO gap is influenced by the chemical structure of the molecule and its environment, the gap separation of the molecules around the NPs decreases. Therefore, the red-shifted is occurred.

In figure (10), the peaks (396-410nm) are corresponding to the emission of TPD because the energy of these peaks is equal to the band gap of TPD 3eV. These peaks appear when using NPs where an Auger-assisted energy due to nano size materials which cause high Auger recombination cross section. When decreasing the TPD, the injected holes across the TPD/ZnO NPs interface decreased, due to the energy offset (~2eV) between the HOMO level of TPD and V.B

ISSN: 2277-3754
ISO 9001:2008 Certified
International Journal of Engineering and Innovative Technology (IJEIT)
Volume 4, Issue 9, March 2015

of the ZnO NPs. While the electrons are efficiently injected in to the C.B of the ZnO NPs. However the energy offset of (~1.8eV) between the ZnO NPs leads to electron accumulation at the TPD/ZnO NPs interface.

Upon accumulation of charges at the heterojunctions interface, the electrons and holes form interfacial charge transfer (CT) excitons, or exciplex states. The energy released from the recombination of these CT excitons is resonantly transferred to the proximal electrons in C.B of the ZnO NPs through an Auger process to produce electrons with sufficiently high energy to inject into the LUMO of TPD. These electrons then radioactively recombine with holes in the HOMO of the polymer, resulting in emission of photons with energy equal to the HOMO—LUMO gap of the TPD. These process described in figure (11). This analysis is identical with [5,14].

B. Chromaticity coordinates and correlated color temperature (CCT)

The light produced by EL and PL, should have an acceptable white color in order to show all the colors of illuminated objects appropriately. Since the color of light is expressed by the CIE colorimetry system, the spectrum of a given light is weighted by the XYZ color matching functions [15]. The resultant three weighted integral values of X, Y and Z are calculated from the luminescence spectrum (EL and PL) by finding the area under the curve for the three region peaks; in red, green and blue region. The chromaticity coordinates x, y on CIE colorimetry system are found from X, Y and Z as follow [16]:

$$x = \frac{X}{X+Y+Z} \qquad (4)$$
$$y = \frac{X}{X+Y+Z}$$

Where X, Y, and Z, which are roughly the area under the curve of the emitted red, green and blue in luminescence spectrum, respectively. Any color of light can be expressed by the chromaticity coordinate (x, y) on the CIE 1931 (x, y) chromaticity. The white light which produced from our 1TPD:1PMMA:0.5%wtZnO NPs at forward bias voltage of 12V has tristimulus coordinates (x, y) = (0.4, 0.32). The correlated color temperature (CCT) for the resulting white light can verified by using McCamy's approximation algorithm to estimate the CCT from the *xy* chromaticities [17].

$$CCT = -449n^3 + 3525n^2 - 6823.3n + 5520.33 \qquad (5)$$

Where

$$n = \frac{x - 0.332}{y - 0.1858} \qquad (6)$$

By using the values of x and y as determined before, the color temperature of the produced white light was found to be about 5000 K. The value of chromaticity coordinates were used in chromaticity diagram as shown in figure (12) to show that the output light of the emission lines registered in EL and PL spectrums is in the white light region and the result for PL was confirmed by photograph of the light emitted from the ZnO NPs solution illuminated by 300nm lamp source as shown in figure (6). The result for EL and PL coordinates are tabulated in table (1).

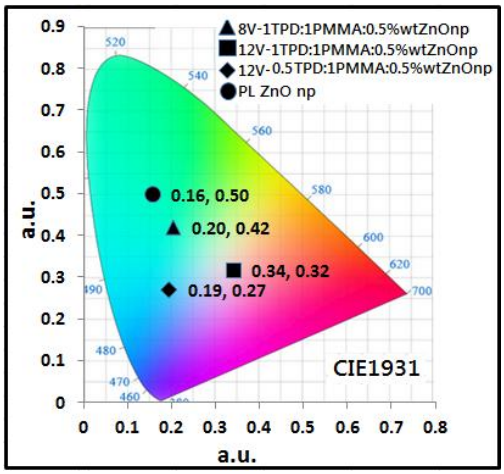

Fig (12): Tristimulus coordinates of ZnO on the CIE 1931 chromaticity diagram

Table (1) :EL and PL coordinates for ZnO NPs.

Component	Excited by	x	y	CCT(K)
1TPD:1PMMA:0.05%wtZnO NPs	biased voltage (12V)	0.35	0.32	5000
1TPD:1PMMA:0.05%wtZnO NPs	biased voltage (8V)	0.28	0.42	10300
0.5TPD:1PMMA:0.05%wtZnONPs	biased voltage (12V)	0.19	0.27	28200
ZnO solution	lamp source (300nm)	0.16	0.5	10500

IV. CONCLUSION

The white light generation from ZnO nanoparticles with organic polymer has been introduced through this research. Our method is significant advantage of lowering the fabrication cost ZnO –based devices. This method benefit from the defect state without the need to use the ZnO nanorods as mentioned in the previous literature survey.

REFERENCES

[1] J.R. Sadaf, M.Q. Israr , O.Nur and M. Willander, " White Electroluminescence Using ZnO Nanotubes /GaN Heterostructure Light – Emitting Diode ", Nanoscale Research Letters, Vol.5, pp.957-960,(2010).

[2] N. Bano, S. Zaman, A. Zainelabdin , S. Hussain , O. Nur and M. Willander, "ZnO-organic hybrid white light

ISSN: 2277-3754
ISO 9001:2008 Certified
International Journal of Engineering and Innovative Technology (IJEIT)
Volume 4, Issue 9, March 2015

emitting diodes grown on flexible plastic using low temperature aqueous chemical method", Journal of Applied Physics, Vol.108, pp.043103,(2010).

[3] R. Guo , J. Nishimura , M. Matsumoto , M. Higashihata , D. Nakamura , T. Okada, "Electroluminescence from ZnO nanowire-based p-GaN/n ZnO heterojunction light-emitting diodes", Appl. Phys. B Vol.94, pp. 33–38, (2009).

[4] A. Zainelabdin ,S. Zaman ,G. Amin ,O. Nur ,M. Willander , "Stable White Light Electroluminescence from Highly Flexible Polymer/ZnO Nanorods Hybrid Heterojunction Grown at 50C", Nanoscale Res Lett ,Vol.5, pp.1442–1448, (2010).

[5] Yuen Yung Hui , Chun-Yu Lee , and Ching-Fuh Lin, " White Light Electroluminescence from Europium Oxide Nanocrystal/Organic Composites", Proceedings of the 7th IEEE International Conference on Nanotechnology, Hong Kong pp.862-865, (2007).

[6] Ching-Fun Lin, Chun-Yu Lee, Yau-Te Haung and Wei-Fang Su, "Electroluminescence from zinc oxide nanoparticles / organic nanocomposites", Appl.Phys.Lett.Vol.89,pp.231116, (2006).

[7] Claudia Pacholski, Andreas Kornowski, and Horst Weller, "Self-Assembly of ZnO: From Nanodots to Nanorods", Angew. Chem. Int. Ed., Vol.41, No.7, pp.1188-1191,(2002).

[8] C.Suryanarayana and M.G.Norton, "X-ray Diffraction A practical Approach" Plenum press. New York, pp.207-221, (1998).

[9] Chun-Yu Lee, Yau-Te Haung, Wei-Fang Su and Ching-Fuhin, "Enhanced ZnO band-gap emission of electroluminescence from ZnO nanoparticles/Organic nanocomposites using a hole-transporting material", Quantum Electronics and Laser Science Conference, Vol.5,pp.1-2,(2007).

[10] Magnus Willander , Omer Nur, Jamil Rana Sadaf, Muhammad Israr Qadir, Saima Zaman, Ahmed Zainelabdin, Nargis Bano and Ijaz Hussain, "Luminescence from Zinc Oxide Nanostructures and Polymers and their Hybrid Devices", Materials, Vol.3, pp.2643-2667, (2010).

[11] S. M. Sze and Kwok K. Ng," Physics of Semiconductor Devices", Third Edition, John Wiley and Sons, New York, (2007).

[12] Thierry Goudon, Vera Miljanovic, and Christian Schmeiser, "On the Shockley-Read-Hall model generation recombination in semiconductors", Society for Industrial and Applied Mathematics, Vol.67, No.4, pp.1183-1201, (2007).

[13] Ijaz Hussain, Nargis Bano, Sajjad Hussain, Yousuf Soomro, Omer Nur and Magnus Willander, "Study of the Distribution of Radiative Defects and Reabsorption of the UV in ZnO Nanorods-Organic Hybrid White Light Emitting Diodes (LEDs)", Materials, Vol.4, pp.1260-1270 , (2011).

[14] Lei Qian, Ying Zheng, Kaushik R. Choudhury, Debasis Bera, Franky So, Jiangeng Xue, Paul H. Holloway, "Electroluminescence from light-emitting polymer/ZnO nanoparticle heterojunctions at sub-band gap voltages" Nano Today, Vol.5, pp.384-389, (2010).

[15] A.M. Suhail, M.J. Khalifa, N.M. Saeed, and Omar.A. Ibrahim, "White light generation from CdS nanoparticles illuminated by UV-LED", Eur. Phys. J. Appl. Phys., Vol.49, pp.30601,(2010).

[16] Janos Schanda "Colorimetry: Understanding the CIE System", first Edition John Wiley,(2008)

[17] C.S. McCamy, "Correlated color temperature as an explicit function of chromaticity coordinates", Color Research & Application Volume, Vol.17, No.2, pp.142-144, (1992).